Microelectronics Journal 88 (2019) 154–163

Contents lists available at ScienceDirect

Microelectronics Journal

journal homepage: www.elsevier.com/locate/mejo

Power adaptive high-resolution neural data compression algorithm (PANDCA)

Mohammed Ashraf [a], Hassan Mostafa [a,b,*], Ahmed Eladawy [a], Yehea Ismail [b]

[a] Electronics and Communications Engineering Department, Cairo University, Giza 12613, Egypt
[b] Nanotechnolgy Department at Zewail City of Science and Technology, New Cairo 11835, Egypt

ARTICLE INFO

Keywords:
Neural signals
Data compression
Image processing
Power harvesting
Low-power design
HW implementation

ABSTRACT

Nowadays, brain scientific research progress depends on signal compression at the implantable site to conform with the low-rate transmission through wireless connection to the outside world despite of high spatial and temporal resolution of neural data. Without data compression, these data rates conflict the neurophysiologic restrictions in terms of energy consumption and silicon area. The main goal of any implantable compression device is to get the smallest data size to be transmitted to the outside world with lowest distortion and data loss at receiver side. In this work, the neural compression algorithm is adapted according to the available harvested power budget. Therefore, the maximum signal to noise and distortion ratio (SNDR) is achieved based on the available harvested power budget without any data loss.

1. Introduction

Neural implantable measurement systems are widely utilized to treat neural disorders as Epilepsy and Parkinson diseases. These neural brain disorders need to be diagnosed and detected, by extracting the complete waveform and history of every electrode instead of extracting some signal features [3]. Besides the need for large number of recording channels, that reaches up to 1024 channels and even more to cover finer spatial resolution of the recordings [12]. These results in large neural data sizes should be transmitted to the outside world.

Thus, a low-power and efficient neural data compression algorithm at the implantable site is very important to be able to transmit these huge neural data to conform with the implantable subsystem requirements such as limited wireless transmission bandwidth with the outside world and low transmitted power.

In neural recording systems, the wireless transmission node is the functional bottleneck in terms of a very limited data rate of a couple of MBit/s [8]. For the transmission of high resolution neural raw data for 1024 electrodes, and electrode resolution of 8-bit with high sampling rate (20 KSample/s/channel), wireless data rates are in order of 160 MBit/s [1]. Correspondingly, powerful and efficient compression algorithm at the implantable site to comply with this huge increase in neural data size is required.

Most of the compression techniques which have been proposed for multichannel neural data are based on the similarity between neural data compression and image compression [2–4,16,18].

Image compression algorithms utilize the spatial correlation between adjacent electrodes only like JPEG and JPEG2000 [9,13,14]. It is obvious that these algorithms are not recommended to be used directly because they are very complex and could not achieve the low-power and the real time restrictions. However, these algorithms should be modified to be suitable for the implantable devices requirements.

In this work, the focus is not on powerful compression algorithms and higher compression ratios only, but also this work considers the hardware efficient (Low-Power and Area-Efficient) algorithms, because power consumption is the main parameter in the implantable devices. In addition, the high sampling rate places a hard restriction on the hardware latency of the target compression algorithm not to violate the real-time processing. Correspondingly, all these restrictions should be combined as design guidelines to select the most suitable compression algorithm.

Therefore, in our previous work [11], the full comparison between main compression algorithms was applied as shown in Fig. 1 and Adaptive 2D-DWT was considered as a most suitable compression algorithm for Low-Power Area-Efficient design due to its hardware simplicity. Despite of that 2D-DCT 8*8 compression algorithm is selected to be used in PANDCA due to its linearity characteristic in the target region as shown in Fig. 1. This characteristic is very important in PANDCA to be able to divide it to equal steps, as described later.

* Corresponding author. Electronics and Communications Engineering Department, Cairo University, Giza 12613, Egypt.
E-mail addresses: mohammedenal@cu.edu.eg (M. Ashraf), hmoustafa@aucegypt.edu, hmostafa@uwaterloo.ca (H. Mostafa), aemira@ieee.org (A. Eladawy).

https://doi.org/10.1016/j.mejo.2018.01.025
Received 19 June 2017; Received in revised form 27 October 2017; Accepted 29 January 2018
Available online 13 February 2018

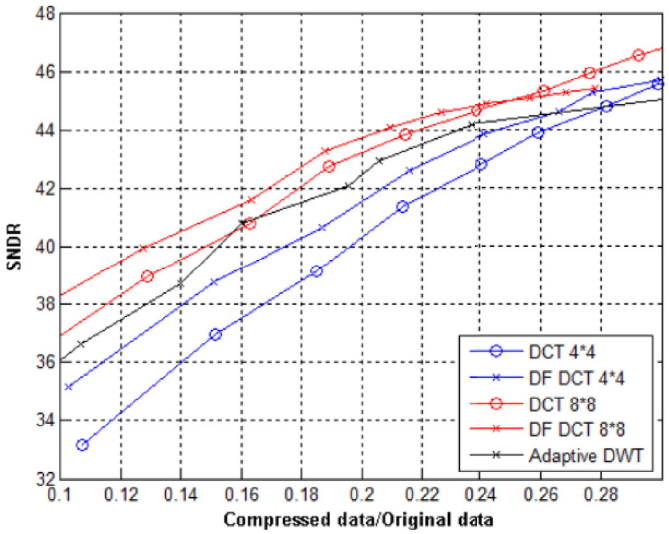

Fig. 1. Performance comparison of the compression algorithms.

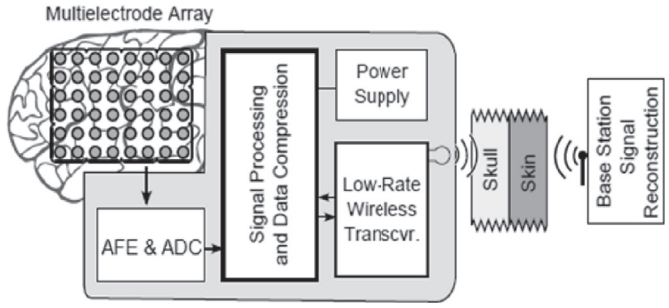

Fig. 2. Neural measurement system full architecture.

Fig. 2 shows the full implantable neural measurement system architecture. This neural system consists of multielectrode array, analog frontend (amplifiers), analog to digital converter, data compression unit, signal processing unit, power supply, and low power wireless transceiver. All these implantable blocks must be low-power, small area, safe on the human body. Neural signals have been recorded from the implantable multielectrode array are amplified in the analog front-end (AFE) and converted to digital neural data using analog to digital (ADC) block. Subsequently, the digital data runs into the main digital module where data compression and signal processing take place. Hence, the low-rate wireless transceiver transmits the compressed neural data to the outside world (reconstruction base station), where signal reconstruction and decompression are performed. Since the system is fully implantable, energy has to be available from implantable power supply (rechargeable battery or harvesting system).

Implantable devices need an efficient power source to supply them with enough energy to power the electrodes, analog interfacing and digital classification as will be described later. Implantable devices are usually powered by a rechargeable battery that is charged by using a micro-scale energy harvesting system. These implantable rechargeable batteries provide the energy for implantable biomedical devices. Devices powered by harvested energy have longer lifetime and provide more comfort and safety than conventional devices. Energies that may be scavenged include infrared radiant energy, thermal energy, vibration energy, body motion energy, wireless transfer energy, and Inductive link energy. Energy harvesting devices generate electric energy from their surroundings through direct energy conversion [5].

In this work, Inductive link harvesting is proposed as the main harvesting source and piezoelectric energy harvesting is proposed as the secondary source.

Inductive link energy harvesting uses wireless transmission of data and power is essentially an air-core transformer which works on the principle of mutual coupling. Primary circuit tuned in series resonance and secondary tuned in parallel resonance.

Piezoelectric energy harvesting uses a direct energy conversion from vibrations and mechanical deformation to electrical energy. This is a promising technique to supply power sources in implantable biomedical devices, since it has higher energy conversion efficiency and a simple structure.

Recently, various technologies, such as advanced materials, micro- and macro-mechanics, and electric circuit design, have been investigated and emerged to improve the performance and the conversion efficiency of the piezoelectric energy harvesters. In this work, the focus is on recent progress of piezoelectric energy harvesting technologies based on PbZrTi (PZT) materials.

Ordinary implantable biomedical devices have 3 scenarios to utilize the available harvested power budget to transmit the compressed neural data to the outside world:

- First scenario is to transmit the neural compressed data with fixed low compression ratio continuously with low rate to guarantee that the minimum available power is enough to transmit the compressed data over all the time.
- Second scenario is to transmit a defined period of neural data when a predefined triggering event occurs such as seizure spikes if there is enough available harvested power budget to transmit this period to the outside world. Otherwise, this triggering event is discarded if there is not enough harvested power budget to transmit this period.
- Third scenario is to send neural data continuously without dependence on any special event with suitable rate as long as there is enough harvested power budget to send it continuously. Otherwise, if there is not enough harvested power budget to continue the transmission, it stops the transmission till producing enough power from harvesting power source then starts the transmission again.

However, all these scenarios are not efficient enough for the current biomedical implantable devices constrains. Current treatment devices need the complete waveform and history for every electrode to be extracted instead of extracting the special signal features only to be able to detect and diagnose neural brain disorders. Accordingly, it should be guaranteed that the detected neural data can be transmitted continuously without any pauses or data loss. In addition, the compressed data can be decompressed at the other side with high quality without significant distortion.

In this work, PANDCA is proposed to use the available harvested power budget to adapt the compression algorithm ratio. Therefore, the proposed technique allows transmitting the compressed neural data continuously. Hence, it achieves maximum signal noise and distortion ratio (SNDR) according to available harvested power budget without any data loss.

The rest of the paper is organized as follows. Section 2 presents the signal characteristics and correlation. Section 3 and Section 4 provide the description and hardware implementation of the proposed compression algorithm and the proposed harvested power adaptive neural data compression algorithm (PANDCA), respectively. Results and a comparison among these different algorithms are discussed in Section 5. Finally the conclusions are drawn in Section 6.

2. Signal characteristics and correlation

To evaluate the performance of the compression algorithms for high resolution neural data, recorded data is used with the same signals characteristics (spatial correlation) of real data, because there is no available high-resolution recorded data with these large sizes and high sampling rates yet. In order to measure the correlation between two signals X_1 and X_2 the Pearson Product-Moment Coefficient is used [19],

as shown in (1).

$$r_{x_1x_2} = \frac{E\left[(x_1 - \mu_{x_1})(x_2 - \mu_{x_2})\right]}{\sigma_{x_1}\sigma_{x_2}} \quad (1)$$

The correlation coefficient $r_{x_1x_2}$ between two random variables X_1 and X_2 with Mean values μ_{x_1}, μ_{x_2} and standard deviations $\sigma_{x_1}, \sigma_{x_2}$.

The degree of correlation is classified in to [3]:

- $0 < |r| < 0.2$: weak correlation
- $0.2 < |r| < 0.5$: medium correlation
- $0.5 < |r| < 1$: strong correlation

The proposed algorithm is applied to the following three sets:

- 64 channels organized in 8×8 grid.
- 32 channels organized in 8×4 grid.
- 16 channels organized in 4×4 grid.

These sets have a strong average spatial correlation between adjacent channels of 0.6130 and maximum of 0.996, and it goes lower when channels are more spatially apart.

In all the transmission rates and power calculations the TI chip CC3100MOD is used as a reference in this work [8]. This chip is a low-power Wi-Fi for Internet of Things (IoT) applications and operates in two modes:

- Standby mode: with current up to 140 μA and average power up to 504 μW.
- Low Power Tx mode: with current up to 223 *m*A and average power up to 802.8 *m*W.

User Datagram Protocol (UDP) transmission mode is used in this work. This protocol is a simpler message-based connectionless protocol. Connectionless protocols do not set up a dedicated end-to-end connection. Communication is achieved by transmitting information in one direction from source to destination without waiting to acknowledge from the receiver. The UDP mode is preferred to be used in independent packets transmission such as sound packets and neural data packets. The proposed reference chip achieves a UDP actual throughput up to 16 Mbps.

In this work, a feedback from the power harvesting device is needed to be able to know the input current level (power level), because PANDCA utilizes it as an input, as will be described later. Hence, a current sensor is adopted to detect the input current level. This input is quantized to suitable number of levels according to the power harvesting device. Then, used as an indicator for the available power level to the compression block.

3. Compression algorithm description and hardware implementation

The proposed compression algorithm is 2D-DCT8x8 Based Compression Method. The neural time instant frame of channels is divided into 8×8 blocks, working from left to right, top to bottom. The 2D-DCT is applied on each block to be converted to frequency representation.

The DCT is one of the most popular compression methods whether in image coding standards such as JPEG or in video coding standards such as MPEG and H.264. Block size 8×8 has high hardware complexity but it has high compression ratio. The DCT equation that computes the $(i,j)^{th}$ entry of the DCT of an image is given by:

$$D(i,j) = \frac{1}{\sqrt{2N}} c(i)\, c(j) \sum_{x,y=0}^{N-1} P(x,y) \cos\left(\frac{\pi(m+1)}{2N}\right) \cos\left(\frac{\pi(n+1)}{2N}\right) \quad (2)$$

With m, n = 0, 1, 2, …,N−1 and c(k) = 1 if $k \neq \{0,N\}$ and $1/\sqrt{2}$ otherwise.

The two-dimensional Discrete Cosine Transform is performed by coefficients matrix multiplication [6].

$$D = T\,P\,T' \quad (3)$$

In (3) matrix P is left multiplied by the DCT coefficients matrix T_{8x8}, as given in Fig. 4, this transforms the rows then multiplied by the transpose of DCT coefficients matrix to transform the columns.

$$\begin{bmatrix} .3536 & .3536 & .3536 & .3536 & .3536 & .3536 & .3536 & .3536 \\ .4904 & .4157 & .2778 & .0975 & -.0975 & -.2778 & -.4157 & .4904 \\ .4619 & .1913 & -.1913 & -.4619 & -.4619 & -.1913 & .1913 & .4619 \\ .4157 & -.0975 & .4904 & -.2778 & .2778 & .4904 & .0975 & -.4157 \\ .3536 & -.3536 & -.3536 & .3536 & .3536 & -.3536 & -.3536 & .3536 \\ .2778 & -.4904 & .0975 & .4157 & -.4157 & -.0975 & .4904 & -.2778 \\ .1913 & -.4619 & .4619 & -.1913 & -.1913 & .4619 & -.4619 & .1913 \\ .0975 & -.2778 & .4157 & -.4904 & .4904 & -.4157 & .2778 & -.0975 \end{bmatrix}$$

Then the 8×8 block of DCT frequency components is ready for quantization, as illustrated in Fig. 3. This stage is the main stage to control the compression ratio and quality level. Quantization is the only lossy stage due to the rounding process, as shown in (4).

$$A = round\left(\frac{D * QL}{Q\_matrix}\right) \quad (4)$$

In (4), a scalar constant Quality Level (QL) is used as a quality controller which changes from 1 to 10. Selecting the QL = 10 provides the highest compression quality, correspondingly the lowest compression ratio and largest transmitted power. On the other side, selecting the QL = 1 provides the lowest compression quality, correspondingly the highest compression ratio and smallest transmitted power. Q_matrix is displayed in Fig. 5.

$$\begin{bmatrix} 16 & 11 & 10 & 16 & 24 & 40 & 51 & 61 \\ 12 & 12 & 14 & 19 & 26 & 58 & 60 & 55 \\ 14 & 13 & 16 & 24 & 40 & 57 & 69 & 56 \\ 14 & 17 & 22 & 29 & 51 & 87 & 80 & 62 \\ 18 & 22 & 37 & 56 & 68 & 109 & 103 & 77 \\ 24 & 36 & 55 & 64 & 81 & 194 & 113 & 92 \\ 49 & 64 & 78 & 87 & 103 & 121 & 120 & 101 \\ 72 & 92 & 95 & 98 & 112 & 100 & 103 & 99 \end{bmatrix}$$

Quantizer output should have a lot of zeros components in the right bottom corner and they decrease gradually to be minimum at the left top side, so that JPEG standard block (ZIGZAG Reorder) is proposed to be used to reorder the components from lower p(0), the probability of having a zero in the matrix field, to higher p(0) to get higher compression

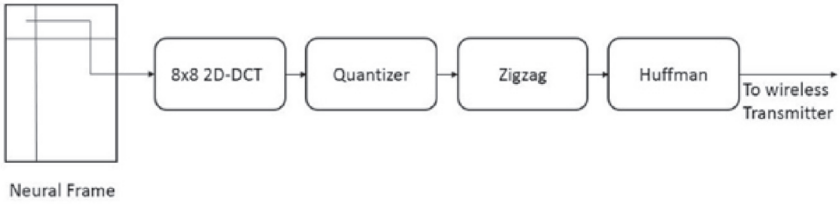

Fig. 3. 2D-DCT8x8 based compression procedure.

$$\begin{bmatrix} .3536 & .3536 & .3536 & .3536 & .3536 & .3536 & .3536 & .3536 \\ .4904 & .4157 & .2778 & .0975 & -.0975 & -.2778 & -.4157 & .4904 \\ .4619 & .1913 & -.1913 & -.4619 & -.4619 & -.1913 & .1913 & .4619 \\ .4157 & -.0975 & .4904 & -.2778 & .2778 & .4904 & .0975 & -.4157 \\ .3536 & -.3536 & -.3536 & .3536 & .3536 & -.3536 & -.3536 & .3536 \\ .2778 & -.4904 & .0975 & .4157 & -.4157 & -.0975 & .4904 & -.2778 \\ .1913 & -.4619 & .4619 & -.1913 & -.1913 & .4619 & -.4619 & .1913 \\ .0975 & -.2778 & .4157 & -.4904 & .4904 & -.4157 & .2778 & -.0975 \end{bmatrix}$$

Fig. 4. T_{8x8} Coefficients matrix.

$$\begin{bmatrix} 16 & 11 & 10 & 16 & 24 & 40 & 51 & 61 \\ 12 & 12 & 14 & 19 & 26 & 58 & 60 & 55 \\ 14 & 13 & 16 & 24 & 40 & 57 & 69 & 56 \\ 14 & 17 & 22 & 29 & 51 & 87 & 80 & 62 \\ 18 & 22 & 37 & 56 & 68 & 109 & 103 & 77 \\ 24 & 36 & 55 & 64 & 81 & 194 & 113 & 92 \\ 49 & 64 & 78 & 87 & 103 & 121 & 120 & 101 \\ 72 & 92 & 95 & 98 & 112 & 100 & 103 & 99 \end{bmatrix}$$

Fig. 5. Q_matrix_{8x8}.

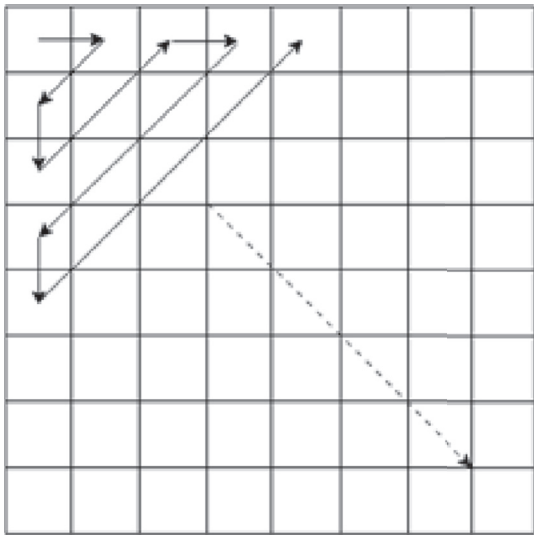

Fig. 6. Zigzag order.

ratio in the Entropy stage, as shown in Fig. 6. The required memory size is 64B to reorder the 8×8 quantized block.

The Entropy stage is a lossless stage that replaces the nonzero components to a stream of binary bits. Huffman coding is a common method to encode the DCT components with variable length codes according to common tables that are assigned according to statistical probabilities. A frequently used symbol will be encoded with a short code, while symbols that are rarely used are represented by a long code.

JPEG standard uses up to 4 tables divided into two sets luminance (DC and AC) and chrominance (DC and AC). In the proposed algorithm, the luminance tables are used because Neural signals DCT components have a similar behavior of luminance DCT components [11].

In order to evaluate the proposed compression algorithm, two performance metrics are used:

- Compression ratio (R): is used to measure the ratio between compressed data size and original data size, as shown in (5).

$$R = \frac{Compressed\ data\ size}{Original\ data\ size} \tag{5}$$

- Signal to Noise and Distortion Ratio (SNDR): is used to measure the quality of reconstruction data $\widehat{D}$ after compression and decompression compared to the original data D [3], as shown in (6).

$$SNDR = 10dB \cdot \log\left(\frac{\|D\|_2^2}{\|D - \widehat{D}\|_2^2}\right) \tag{6}$$

- Structural Similarity: is used to measure the similarity between original frame and reconstructed frame [20].

4. Harvested power adaptive algorithm (PANDCA)

4.1. Neural system power source

Rechargeable batteries which used in implantable medical devices should be continuously charged. PANDCA implantable system harvests its power using two sources: main source (inductive link) fixed on the same place of battery and secondary source (piezoelectric) fixed on the heart.

Inductive link for wireless transmission of data and power is essentially an air-core transformer which works on the principle of mutual coupling. Primary circuit tuned in series resonance and secondary tuned in parallel resonance as shown in Fig. 7. Inductive powering for implanted medical devices is a safe and effective technique that allows power to be delivered to implants wirelessly. Wireless powering is very sensitive to a number of link parameters, including coil distance, alignment, shape, and load conditions. The optimum drive frequency of an inductive link varies depending on the coil spacing and load. Efficient model provides practical results 100 mW output power at 2.5 MHz [21]. Inductive link is the main power provider to our implantable system.

Piezoelectric energy harvesting technologies based on PbZrTi (PZT) materials which have the most outstanding piezoelectric properties, and powered by mechanical energy from a patient's own heart beats. Volture product is used as a reference in this work [22]. Piezoelectric material produces mechanical strain under the influence of an externally applied

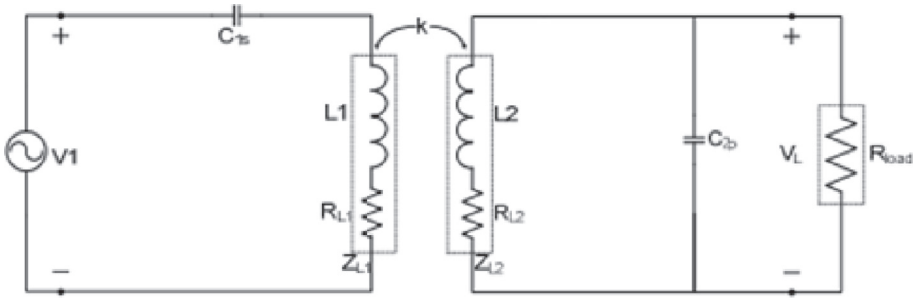

Fig. 7. Inductive link topology.

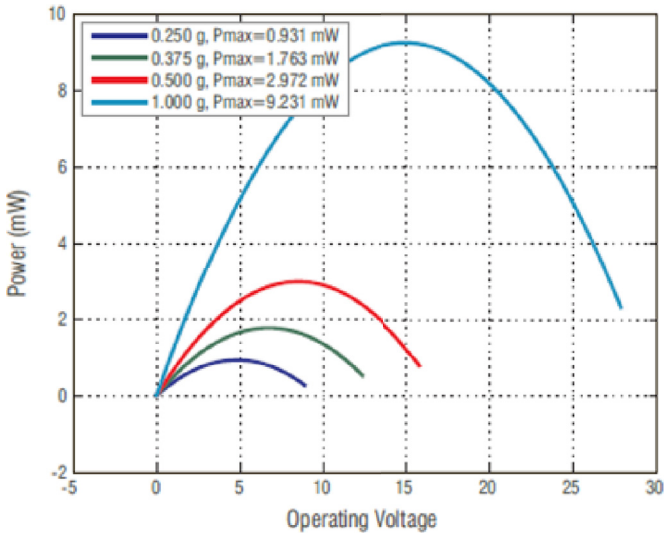

Fig. 8. Piezoelectric performance [22].

electrical field, and conversely produces electrical potential in response to applied mechanical strain. Products such as the Volture piezo energy harvester are typically used in a cantilevered-beam configuration, in which the piezoelectric beam is clamped at one end and the other end allowed to oscillate freely in response to vibration normal to the flat surface of the beam, converting these vibrations to in-plane material strain. The beam dimensions and tip mass determine the resonant frequency of the beam, which is tuned to match the dominant vibrational frequency of its environment, mechanically amplifying this typically small vibration. The vibration frequency being generated by the shaker was then matched to the frequency of the Volture product to provide resonant and therefore optimized energy harvesting. Fig. 8 shows the power against operating voltage at four different amplitudes (0.25, 0.375, 0.5, and 1.00 g) and frequency 40 HZ.

4.2. Neural system power tree

The main power hungry blocks in neural implantable devices are the wireless transmitters [10] and the data compressors [11]. Thus, the large percentage of the harvested power budget is dedicated to the wireless transmitter and compression block as shown in Fig. 9.

4.2.1. Compression block power

If the number of channels (electrodes) is constant, compression block consumes constant power regardless of the compression ratio. After RTL Hardware Implementation on 130 nm technology for ASIC implementation, PANDCA consumes 32.06 mW. This power consumption is drawn from the power budget as a constant value and the remaining power budget is used by the wireless transmitter.

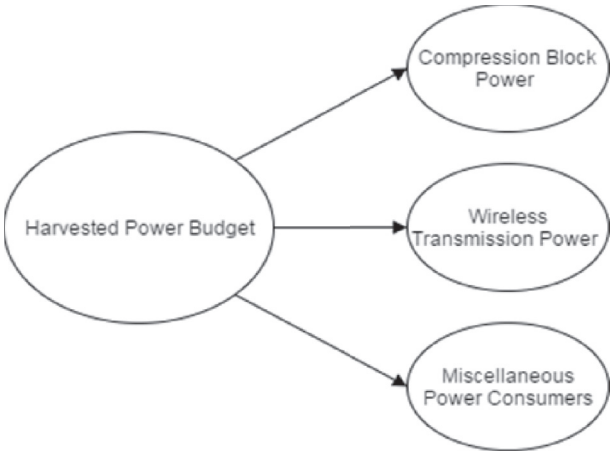

Fig. 9. Neural system power tree.

4.2.2. Miscellaneous power consumers

Neural Implantable devices have a lot of blocks which consume power such as electrodes, analog interfacing, and digital controllers. However, the main characteristic which combines them is that they consume fixed power regardless any change in quality factor. So this power consumption is drawn from the power budget too as a constant value and the remaining power budget is used by the wireless transmitter.

4.2.3. Wireless transmission power

Low power WIFI chips support data rates up to 16 Mbps. The TI chip CC3100MOD in transmission only mode is always sleep except when there is available data to be transmitted. In sleep mode, the absorbing current consumption is very small compared to transmission mode so that it can be negligible.

Therefore, the power consumption duration is in the TX mode duration only. Hence, the size of data to be transmitted is the main parameter in power consumption. When this data size increases, the duration of Tx mode increases, so is the current (power) consumption. On the other hand, when this data size decreases, the duration of the Tx mode decreases so is the current (power) consumption as shown in Fig. 10.

As shown in (7), absorbing current (power) is linearly proportional with time.

$$P = VI = V\left(\frac{V}{R}.t\right) = \left(\frac{V^2}{R}\right).t \tag{7}$$

In this work, data size is assumed to be linearly proportional to the duration of transmission (absorbed Power), assuming that the traffic is idle, especially because TI WIFI chip is used in UDP mode [8]. Hence, absorbing power can be controlled according to compressed data size.

4.3. Quality Factor Effect

In the proposed compression algorithm, the quality of compressed data (SNDR) is controlled according to quality factor which varies from 1 to 10. This range is selected because SNDR is approximately linearly proportional with quality factor in this range only, as shown in Fig. 11 and this characteristic is important in the proposed PANDCA as will be analyzed. Hence, there are 10 quality levels and according to this quality factor change, the compressed data size changes.

As shown in Fig. 11, when the quality factor increases, the compression ratio (compressed data size divided by original data size) increases and vice versa. On the other hand, when the quality factor increases, the SNDR increases and vice versa. Hence, the output compressed data size can be controlled and its quality (SNDR) according to quality factor level.

Fig. 12 shows the structure similarity between original frame and reconstructed frame at smallest quality factor (quality factor 1) and largest quality factor (quality factor 10).

4.4. PANDCA architecture

As shown in Fig. 13, this is the proposed algorithm to control the compression algorithm quality factor (compressed data size) according to available harvested power budget:

1. Subtract the needed power for the compression block and other needs from the total available harvested power budget to get the available power budget to transmit the compressed data.

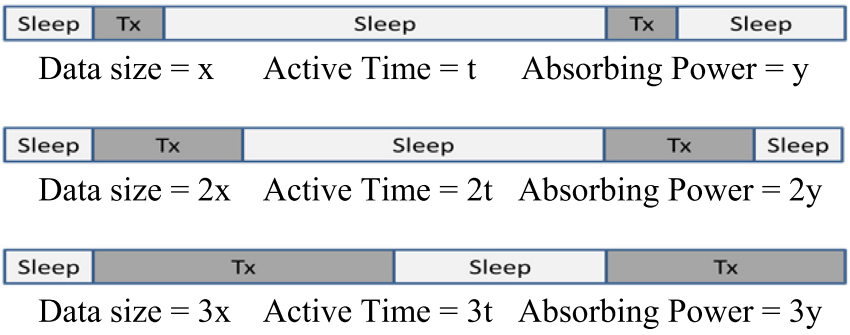

Fig. 10. Transmission timing scheduling [8].

2. Select the size of compressed data which can be transmitted with this available power (according to WIFI chip specifications).
3. Calculate the needed compression ratio (needed size of compressed data/size of original data).
4. Select the initial quality factor from the saved data in Table 1, this data is obtained from the previous results with the same correlation, resolution and number of electrodes (channels). This table should be recalculated if any parameter is changed.
5. If the actual compressed data size is equal to, or less than, the suggested compressed size with a specific limit, the compression algorithm should continue with the same quality factor in the next frames.
6. If it is larger than the calculated size or less with a specific limit, the compression algorithm will increment or decrement the quality factor level with quantized steps according to the error step size.
7. The selected quality factor will be in use until the power harvested budget is changed. Once the available harvested power budget is changed repeat again from step 1.

4.5. PANDCA HW implementation

Fig. 14 shows the HW implementation of PANDCA algorithm. In order to get hardware area and hardware power, the following steps are conducted:

- Synthesis analysis is made by design compiler (Synopsys tool). A synthesis tool takes the RTL hardware description and a standard cell (130 nm) library as input and produces a gate-level netlist as output. The resulting gate-level netlist is a completely structural description with only standard cells at the leaves of the design. Internally, a synthesis tool performs many steps including high-level RTL optimizations, RTL to unoptimized boolean logic, technology independent optimizations, and finally technology mapping to the available standard cells.

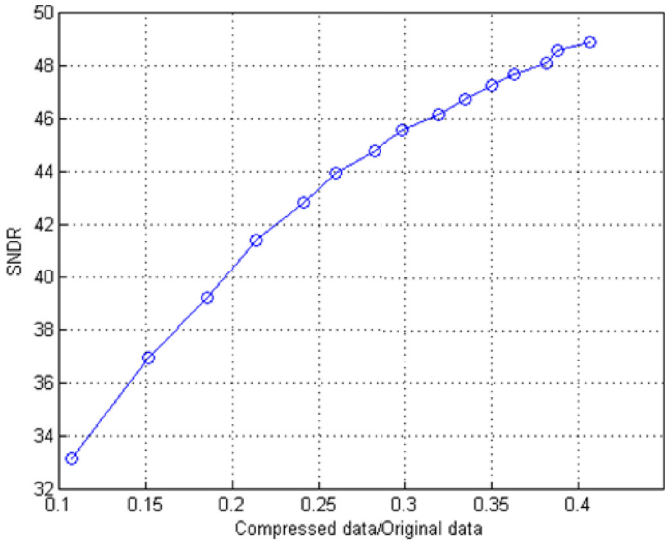

Fig. 11. Quality factor effect.

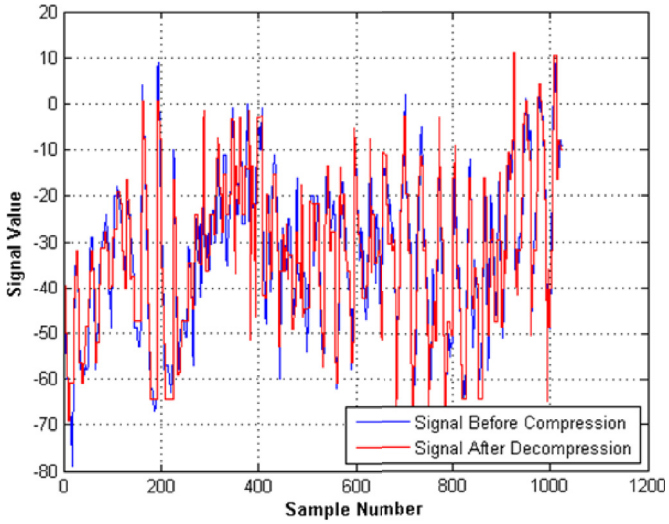

(a) Smallest Quality Factor

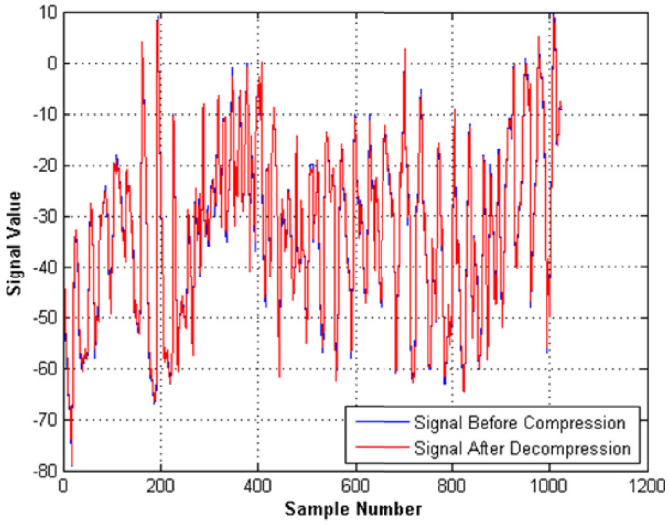

(b) Largest Quality Factor

Fig. 12. Structural similarity.

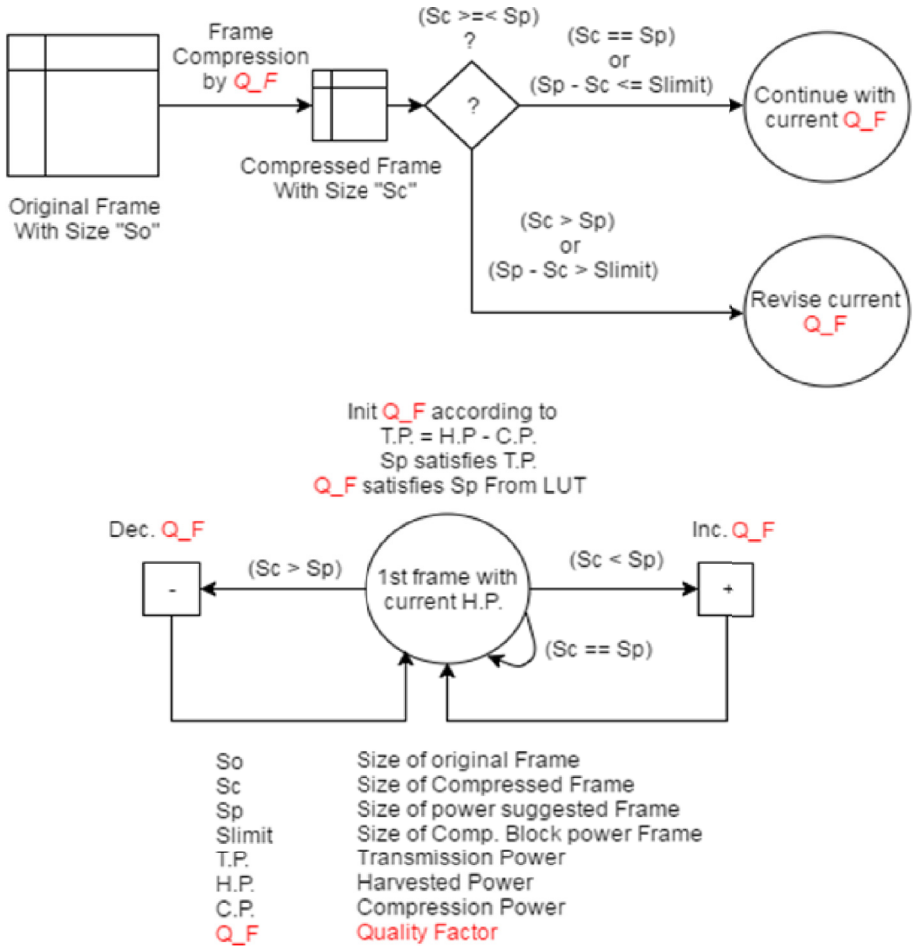

Fig. 13. Harvested power adaptive design.

Table 1
64-Channel results.

Q_F Index	Sp (Byte)	Frame rate (KBps) ch. rate = 20 Ksps	Tx. Duration per (1s) with rate 16 Mbps (ms)	Tx. Power (mW)
1	4	80	40	32.11
2	7	140	70	56.2
3	9	180	90	72.25
4	10	200	100	80.28
5	11	220	110	88.31
6	12	240	120	96.34
7	13	260	130	104.36
8	14	280	140	112.39
9	15	300	150	120.42
10	16	320	160	128.45

- The area of the hardware design is measured on 130 nm technology for ASIC implementation. Hence, the needed SRAM memory for every compression algorithm is calculated and multiplied by 6-transistor SRAM area for the same technology.

	PANDCA
Area (μm)	728633
Power (mw)	96.94
Latency Per Frame (clock cycle)	3280

5. Results and discussion

The (64-channel) results are discussed and explained in details. Then, the other channel resolutions results are provided and compared to (64-channel) results.

Table 1 shows the suggested initial saved values to start with at step 4 according to available power budget to transmit. Then, go up and down in the next frames according to error step, this table is for (64-channels) results:

Column 1 divides the quality factors to 10 levels from 1 to 10, when the quality factor increases, the SNDR increases and the compressed data size increases.

Column 2 is the compressed frame sizes according to quality factor level. It is calculated after hundreds of trials on the brain neural data.

Column 3 is the frame (64-channel) sampling rate if the channel (electrode) rate is 20 Ksps.

Column 4 is the needed transmission duration per one second with transmission rate 16 Mbps.

Column 5 is the needed transmission power if the sleep duration is ignored according to the reference TI WIFI chip CC3100MOD transmission current and voltage.

All these values should be changed if any parameter from electrodes resolution, electrodes correlation, electrode sampling rate, number of channels, transmission rate or WIFI chip is changed.

Fig. 15 shows four cases of available harvested power budget profile and the performance of the proposed PANDCA based on the harvested power scenario.

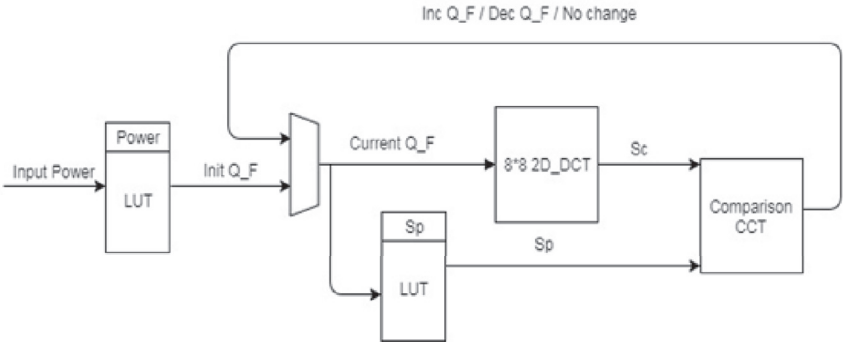

Fig. 14. PANDCA HW implementation.

Constant harvesting power profile (Fig. 15a):

In this case, the available harvested power budget to transmit is 90 mW and it is fixed on this value over all the duration.

The proposed PANDCA searches on the nearest power entry on the saved table (Table 1), and selects entry number 6 as an initial value, because it is the lower nearest entry from available power.

To achieve this target power of 88.3 mW, the proposed compression algorithm needs to be adapted initially to quality factor level 5, to get compressed frame size around (11 B), frame rate around (220 Kbps) and transmission duration around .11 s to get the target power of 88.3 mW.

After starting with quality factor level 5, a compressed size (11 B), and this value is lower than the suggested size acceptable range, then it increases the quality factor to level 6 at the next frame trying to enter this acceptable range.

In the second frame, a compressed size (12 B), and this value is more than suggested size acceptable range, then it decreases the quality factor to level 6 again at the next frame trying to enter this acceptable range. This continues till entering the acceptable range and settles the quality factor level or continues in trying mode around the acceptable range.

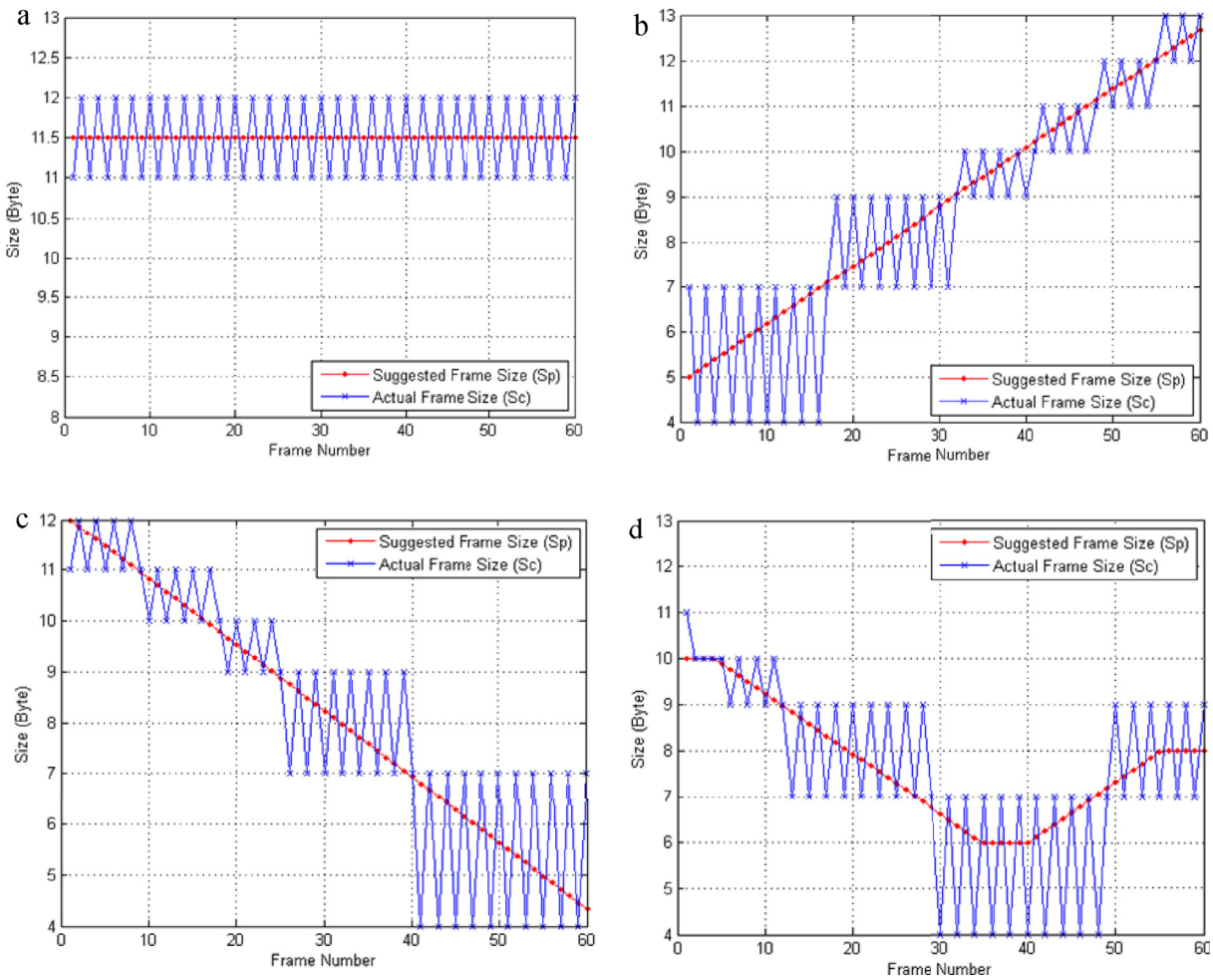

Fig. 15. a: Constant Power Adaptive Performance. b: Increasing Power Adaptive Performance. c: Decreasing Power Adaptive Performance. d: Real Power Adaptive Performance.

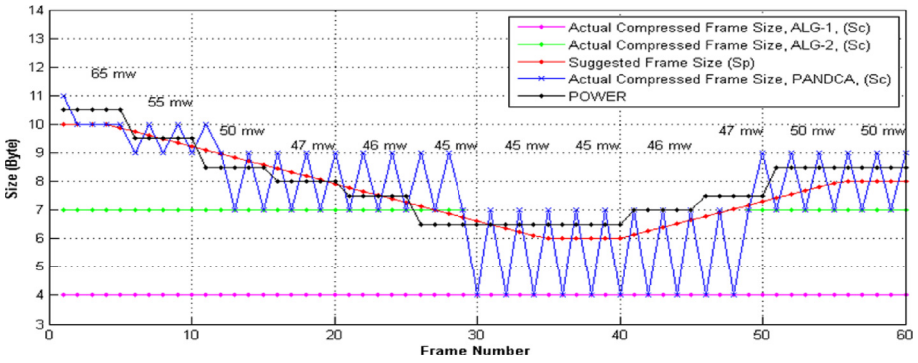

Fig. 16. Power performance comparison.

Table 2
32-Channel results.

Q_F Index	Sp (Byte)	Frame rate (KBps) ch. rate = 20 Ksps	Tx. Duration per (1s) with rate 16 Mbps (ms)	Tx. Power (mW)
1	2	40	20	16.06
2	4	80	40	32.11
3	4.5	90	45	36.12
4	5	100	50	40.14
5	5.5	110	55	44.15
6	5.6	112	56	44.96
7	5.7	114	57	45.76
8	6	120	60	48.17
9	6.5	130	65	52.18
10	7.5	150	75	60.21

Table 3
16-Channel results.

Q_F Index	Sp (Byte)	Frame rate (KBps) ch. rate = 20 Ksps	Tx. Duration per (1s) with rate 16 Mbps (ms)	Tx. Power (mW)
1	1	20	10	8.03
2	1.25	25	12.5	10.04
3	2	40	20	16.06
4	2.1	42	21	16.86
5	2.25	45	22.5	18.06
6	2.5	50	25	20.07
7	2.75	55	27.5	22.08
8	3	60	30	24.08
9	3.25	65	32.5	26.1
10	3.5	70	35	28.1

Increasing harvesting power profile (Fig. 15b):

In this case, the available harvested power budget to transmit at the first frame is 60 mW and it is increasing linearly over all the duration.

The proposed PANDCA searches on the nearest power entry on the saved table (Table 1), and selects entry number 2 as an initial value, because it is the lower nearest entry from available power.

To achieve this target power of 56.2 mW, the proposed compression algorithm needs to be adapted initially to quality factor level 2, to get compressed frame size in around (7 B), frame rate around (140 Kbps) and transmission duration around .07 s to get the target power of 56.2 mW.

After starting with quality factor level 2, a compressed size (7 B), and this value is more than suggested size acceptable range, then the quality factor is decreased to level 1 at the next frame trying to enter this acceptable range.

In the second frame, the proposed compression algorithm faces increase in the available harvesting power level, then the new comparison will be against larger suggested power due to this increase, but this increase can be handled by increasing the quality factor level trying to enter this acceptable range. This continues till entering the acceptable range and settles the quality factor level or continues in trying mode around the acceptable range.

Decreasing harvesting power profile (Fig. 15c):

This case has a similar behavior like Fig. 15 b behavior, but on opposite direction.

Real harvesting power profile (Fig. 15d):

In this case, the available harvested power budget to transmit at the first frame is 90 mW and it varies continuously over all the duration. Correspondingly, the proposed PANDCA tries to adapt the quality factor level to overcome these rapid changes on the available harvested power budget as shown in Fig. 15 d.

As shown on these four case studies, the proposed (PANDCA) achieves the highest possible SNDR based on the available harvested power budget.

In Table 4 and Fig. 16, the comparison between conventional algorithm (Alg-1) which compresses the neural data with fixed compression ratio to be able to produce a suitable compressed data size to be transmitted to the outside world without any discontinuity when power level decreases to the lowest level against the proposed PANDCA. On the other side, despite of conventional algorithm (Alg-2) uses the intermediate quality factor to achieve accepted SNDR all over the time, it faces a suddenly discontinuity once the available power budget decreases than the enough amount to transmit the compressed data. It is obvious that there is a significant enhanced performance of the proposed algorithm compared to the conventional algorithm especially in cases (b, c and d) because the harvested power is variable with time and conventional algorithms are not adaptive to these cases. Knowing that normally in the implantable devices for neural data compression, the harvested energy exhibits different profiles based on the environmental conditions.

Table 4
Performance comparison.

	Constant Power (case a)		Increasing Power (case b)		Decreasing Power (case c)		Real Power (case d)	
	Avg. SNDR	Number of Tx Bytes per 60 Frame	Avg. SNDR	Number of Tx Bytes per 60 Frame	Avg. SNDR	Number of Tx Bytes per 60 Frame	Avg. SNDR	Number of Tx Bytes per 60 Frame
Conventional Compression Algorithms Alg-1	40	660	34	240	34	240	34	360
Power Adaptive Algorithm	41	690	38	520	36	492	38	451

Tables 2 and 3 show the results for two other model sizes (32-channels) and (8-channels) respectively with high resolution grid too, these small model sizes are compressed with 2D-DCT as well but with 4×4 block size.

Finally, the harvested power adaptive high-resolution neural data compression algorithm (PANDCA) is the most suitable compression algorithm for low-power implantable devices for neural data compressing. To reconstruct the data without performance degradation, higher possible SNDR over all the time should be achieved and the only obstacle to achieve that is the available harvested power.

Correspondingly, the best method to achieve the highest possible SNDR based on available harvested power budget is to control the compression algorithm based on the available harvested power.

6. Conclusion

Neural data research has a wide application today and it heavily depends on data compression to be able to extract all signal waveforms with finer resolution for further processing. This work proposes a harvested power adaptive high-resolution neural data compression (PANDCA) as the most suitable compression algorithm candidate to achieve the highest possible SNDR based on available harvested power budget without any data loss or discontinuity in the transmission to the outside world.

Acknowledgment

This work was partially funded by Cairo University, Zewail City of Science and Technology, NTRA, ITIDA, ASRT, Mentor Graphics, NSERC.

References

[1] S. Schmale, B. Knoop, J. Hoeffmann, D. Peters-Drolshagen, S. Paul, Joint compression of neural action potentials and local field potentials, in: 47th Asilomar Conference on Signals, Systems and Computers, Nov 2013, pp. 1–4.

[2] T. Kim, N.S. Artan, J. Viventi, H.J. Chao, Spatiotemporal compression for efficient storage and transmission of high-resolution electrocorticography data, in: Annual International Conference of the IEEE Engineering in Medicine and Biology Society, 2012, pp. 1–4.

[3] S. Schmale, J. Hoeffmann, B. Knoop, G. Kreiselmeyer, H. Hamer, D. Peters-Drolshagen, S. Paul, Exploiting Correlation in Neural Signals for Data Compression, November 2014, pp. 1–4.

[4] C. Chung, L. Chen, Y. Kao, F. Jaw, Multichannel Evoked Neural Signal Compression Using Advanced Video Compression Algorithm, May 2009, pp. 1–4.

[5] M. Billinghurst, T. Starner, Wearable devices. New ways to manage information, IEEE J. Mag. (Computer) 329 (1) (1999) 57–64.

[6] Min-Gyu Kang, Woo-Suk Jung, Recent Progress on PZT Based Piezoelectric Energy Harvesting Technologies, 2016, pp. 1–4.

[8] http://www.ti.com/product/CC3100MOD.

[9] B. Usevitch, A tutorial on modern lossy wavelet image compression: foundations of JPEG, in: Signal Processing Magazine, vol. 18, IEEE, 2000.

[10] A. Yakovlev, S. Kim, Implantable Biomedical Devices: Wireless Powering and Communication, April 2012, pp. 1–4.

[11] M. Ashraf, H. Mostafa, A Low-power Area-efficient Design and Comparative Analysis for High-resolution Neural Data Compression, Dec. 2017, pp. 1–4.

[12] M. Asenwi, T. Ismail, H. Mostafa, Performance analysis of hybrid lossy/lossless compression techniques for EEG data, in: IEEE International Conference on Microelectronics (ICM 2016), IEEE, Cairo, Egypt, 2016, pp. 1–4.

[13] S. Fauvel, Ward, An energy efficient compressed sensing framework for the compression of electroencephalogram signals, Sensors 14 (1) (2014) 1474–1496.

[14] G. Antoniol, P. Tonella, Eeg data compression techniques, Biomed. Eng. IEEE Trans. 44 (2) (1997) 105–114.

[16] S. Akhter, M. Haque, Eeg compression using run length encoding, in: Signal Processing Conference, 2010 18th European, IEEE, 2010, pp. 1645–1649.

[18] B.A. Rajoub, An efficient coding algorithm for the compression of eeg signals using the wavelet transform, Biomed. Eng. IEEE Trans. 49 (4) (2002) 355–362.

[19] L. Fahrmeir, R. Künstler, I. Pigeot, G. Tutz, Statistik: Der Weg zur Datenanalyse, 2007, pp. 1–4.

[20] Zhou Wang, A.C. Bovik, H.R. Sheikh, E.P. Simoncelli, Image quality assessment: from error visibility to structural similarity, in: IEEE Transactions on Image Processing, vol. 13, April 2004, pp. 600–612, 4.

[21] H. Ali, T.J. Ahmad, S. a Khan, Inductive link design for medical implants, in: 2009 IEEE Symposium on Industrial Electronics & Applications, Oct. 2009, pp. 694–699 no. Isiea.

[22] http://www.tande.com.tw/eh-energy-harvesting.